Polymer 51 (2010) 5332–5344

Contents lists available at ScienceDirect

Polymer

journal homepage: www.elsevier.com/locate/polymer

Coupling onto surface carboxylated cellulose nanocrystals

Nadège Follain*,[1], Marie-France Marais, Suzelei Montanari, Michel R. Vignon

Centre de Recherches sur les Macromolécules Végétales, (CERMAV-CNRS), affiliated with the Joseph Fourier University, BP 53, 38041 Grenoble Cedex 9, France

ARTICLE INFO

Article history:
Received 8 April 2010
Received in revised form
30 August 2010
Accepted 1 September 2010
Available online 17 September 2010

Keywords:
Surface carboxylated cellulose nanocrystals
Solid-state NMR spectroscopy
EPR spectroscopy

ABSTRACT

Non-flocculating aqueous suspensions of cellulose nanocrystals with different sizes were prepared by the combination of acid hydrolysis and surface TEMPO oxidative carboxylation of cotton linter and microfibrils of parenchyma cell cellulose (PCC). A decrease of the crystal size occurred and the introduction of negative charges at the interface of the crystalline domains induced a better individualization of the crystallites. These suspensions were further amidated by interaction with 4-amino TEMPO; a nitroxide radical containing a terminal amino group. The products were characterized by elemental analysis, conductimetry, solid-state ^{13}C NMR, FTIR and EPR spectroscopies, together with X-ray diffraction analysis and the coupling performance was deduced with a high correlation. The results indicated that the amidation was effective with yield roughly of 30%, the reaction yield being somewhat more important on samples from cotton origin. In all samples, the amidation was realized at the surface of the samples from carboxylated functions, which kept their intrinsic crystallinity, integrity and perfection throughout the preparation protocol. Their hydrophobic character was evaluated by observing their behavior in polar and non-polar solvents.

1. Introduction

With the current incentive to produce polymer-based materials from sustainable resources, the abundant and renewable cellulose stands out as choice candidate to fulfill this demand. Besides the classical uses of cellulose in the field of textile, paper and derivatives industries, new developments based on the advantageous utilization of the unique ultrastructural morphology of cellulose are pursued. Indeed at the sub micrometer level, all cellulose containing organisms display an assembly of microfibrils of few nanometers in width and many micrometers in length. In view of their ubiquity, it is commonly accepted that the microfibrils are the basic building blocks of all cellulose materials [1–4]. The occurrence of the microfibrils takes its origin in the mode of cellulose biosynthesis, whereby enzymatic spinnerets, commonly called terminal complexes, extrude slender microfibrils of uniform diameter, that result from the continuous biopolymerization, spinning and crystallization of nearly endless cellulose molecules [2]. The perfection of this enzymatic machinery is such that within any given cellulose microfibrils, the chains are fully extended, and there is only a limited number of defects along the microfibrillar length [5,6]. After an acid treatment, the microfibrils become cut longitudinally at their defects, with the result of shorter elements: the cellulose nanocrystals [1]. These nanocrystals have the same diameter as the initial microfibril, but lengths ranging from tenth of nanometer for samples from wood or cotton origin to several micrometers for tunicin or Valonia cellulose. It is generally accepted that these nanocrystals consist of fully extended cellulose chain segments well organized in perfect crystalline arrangement. Typically, these nanocrystals sometimes named “cellulose whiskers”, display mechanical properties that approach the theoretical value of perfect cellulose crystal, with a modulus close to 150 GPa and strength of the order of 10 GPa [7–9]. These high values, together with the abundance and renewability of cellulose has been attracting a great interest for their incorporation as reinforcing agents in bio-based composites and nanocomposites [10].

It is as early as 1991 that in a first report, it was observed that a substantial reinforcement effect was obtained by impregnating tunicin – animal cellulose – nanocrystals mats with water-soluble thermosetting resins [11]. Following this early results, it was further revealed that an adequate mixing of small amounts of non-flocculated aqueous suspensions of cellulose nanocrystals with aqueous solutions or suspensions of polymers, followed by drying of the mixture could lead to a drastic increase in the physical properties of the resulting nanocomposites [12]. This effect was particularly spectacular above the Tg of the polymer matrix, as it was shown that the reinforcing effect could be maintained until the softening

* Corresponding author. Tel.: +33 235 14 66 98; fax: +33 235 14 67 04.
E-mail address: nadege.follain@univ-rouen.fr (N. Follain).
[1] Present address: Laboratoire “Polymères, Biopolymères et Surfaces”, Université de Rouen, UMR6270 & FR3038 CNRS, 76821 Mont-Saint-Aignan cedex, France.

0032-3861/$ – see front matter © 2010 Elsevier Ltd. All rights reserved.
doi:10.1016/j.polymer.2010.09.001

temperature of cellulose [13]. A major drawback of these results is that in order to get homogenous dispersions of the cellulose elements within the nanocomposites, the reinforcing nanocrystals need to be initially surface sulfated or carboxylated in order to be handled as non-flocculated aqueous suspensions [13,14]. In most apolar organic solvents, these suspensions invariably flocculate and are therefore not suited to be homogenously dispersed in the solutions of most commodity polymers. To circumvent this hurdle many studies have been devoted to modify the skin of the cellulose nanocrystals in order to render them hydrophobic, without affecting the integrity of their cores and thus keeping the initial mechanical properties of the corresponding nanocrystals. After modifications these hydrophobic nanocrystals become dispersible, without flocculation in apolar solvents and can thus be homogenously incorporated in most polymers. For this, typical modifications range from the selective adsorption of surfactant [15] to the chemical derivatization of cellulose surface hydroxyl groups [16,17].

This work was undertaken in this context. We have taken advantage of the possibility to convert the surface hydroxymethyl groups of cellulose nanocrystals into carboxyl groups, following the classical TEMPO-mediated oxidation reaction [18–20]. It was shown that these surface carboxylated nanocrystals could be further modified by an amidation coupling with a series of amines using water-soluble carbodiimide, thus giving the possibility to modify the hydrophilic/hydrophobic surface property of the cellulose nanocrystals, using amines presenting hydrophilic or hydrophobic moieties. So far, only few reports have described the details of such coupling [20–22]. Here, we have followed such amidation reaction on nanocrystals from cotton linters and from sugar beet pulp cellulose, by using 4-amino TEMPO as a probe [22]. The quantification of the coupling reaction was achieved by a using a series of spectroscopic analyses as well as other analytical tools. In particular, the nitroxide moiety of the probe was found very valuable to quantify the coupling reaction accurately and unambiguously by analyzing the electron paramagnetic resonance spectroscopy data from the modified samples.

2. Experimental section

2.1. Materials

2.1.1. Chemicals

TEMPO, 4-amino TEMPO, sodium bromide and sodium hypochlorite were purchased from Aldrich whereas N-(3-Dimethylaminopropyl)-N′-ethylcarbodiimide hydrochloride (EDC) and N-hydroxysuccinimide (NHS) were obtained from Sigma.

2.1.2. Cellulose

Two cellulose samples were used in this work, (i) a batch of cotton linters from Tubize Plastics, Rhodia (Belgium), which was used as received and (ii) a sample of dried parenchyma cell cellulose (PCC) from sugar beet pulp (SBP) from General Sucrière Saint Louis Sucre (Nassandres, France). This last sample was desincrusted according to the procedure of Dinand et al. [23] and dispersed in water with a Waring Blender operated at full speed for 5 min at a concentration between 1% and 2% (w/v). The slurry which had reached a temperature of 60 °C was immediately further treated in a laboratory scale Manton–Gaulin homogenizer 15MR-8TBA, from APV Gaulin Inc., Wilmington, Mass. Fifteen passes were applied using a pressure of 500 bar and keeping the temperature below 95 °C to avoid cavitation. The resulting creamy suspension did not flocculate as it was stabilized by the presence of charged glucuronic and galacturonic acid residues at the microfibril surfaces, as already published [24,25]. The suspension was either freeze-dried or kept at 3–4 °C for further use.

2.1.3. HCl hydrolysis

20 g of cotton linters or 16 g (based on dry weight) of dispersed PCC from SBP were hydrolyzed with 1 L of 2.5 M HCl at 100 °C for 20 min to yield suspensions of cellulose nanocrystals, which were filtered and washed with water until neutral pH. The weight loss resulting from the hydrolysis step was around 10% for cotton linters and 20–25% for PCC from SBP. For both samples, this product loss corresponded to the hydrolysis of the cellulose amorphous zones, as already transcribed in the literature, in particular by Araki et al. [20] and Montanari et al. [26]. In addition, for PCC from SBP, the additional product loss was due to the removal of the residual hemicellulose and pectic polysaccharides located at the surface of the microfibrils [24,25]. In the text, these samples are named cellulose nanocrystals indexed to their cellulose origin.

2.1.4. TEMPO-mediated oxidation

Oxidation experiments, schematized in Fig. 1, were carried out as previously published [27,28] with minor modifications [22].

In a typical run, cellulose samples (1.95 g, 12 mmol anhydro glycosyl units or AGU) were dispersed in distilled water (180 mL) for 3 min with a high speed T25 basic Ultra-Turax homogenizer (Ika-Labortechnik, Staufen, Germany). 90 mL of water, which was used to wash the homogenizer, was then added to the suspension. TEMPO (30 mg, 0.19 mmol), NaBr (0.63 g, 6.1 mmol) and NaOCl (1.76 M solution, 1.5 mL, 2.64 mmol) was stirred in 20 mL of water until complete dissolution. This solution was then added to the cellulose

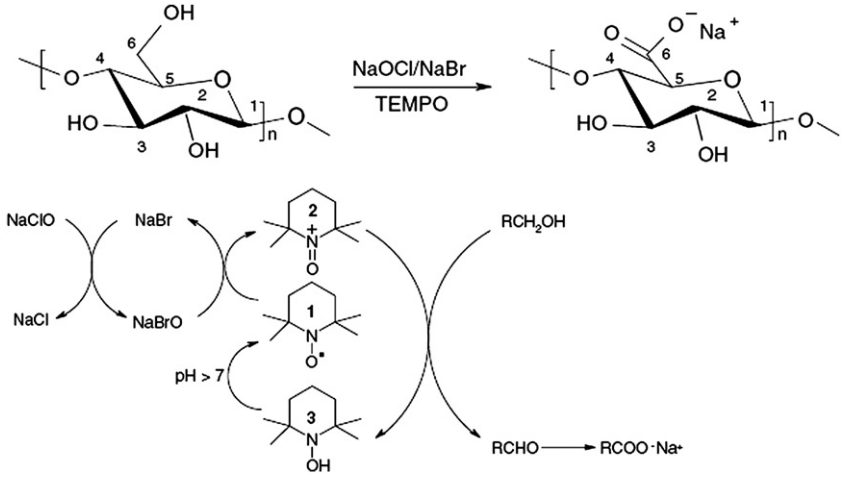

Fig. 1. Oxidation scheme of cellulose with TEMPO mediation [28].

suspension, which was mechanically stirred and maintained at 20 °C. The NaOCl (1.76 M solution, 11.5 mL, 20.24 mmol) was added dropwise to maintain the pH at 10 during the addition. After the total addition of NaOCl, the pH was maintained constant at 10 by adding 0.5 M NaOH solution until no more variation was observed, indicating the end of the reaction. Methanol (5 mL) was then added to destroy the residual NaOCl and the pH was adjusted to 7 with 0.5 M HCl. The resulting white suspension was further separated by centrifugation, yielding a supernatant consisting of water-soluble oxidized cellulose derivative, and a pellet corresponding to surface carboxylated cellulose nanocrystals. This fraction was further purified by successive centrifugation, re-dispersion in water and finally by dialysis against distilled water. Its final yield was about 92–95% for the sample from cotton linters and 88–92% for the one from microfibrillated PCC from SBP.

2.1.5. Coupling reaction

The coupling between carboxylated cellulose nanocrystals and 4-amino TEMPO is schematized in Fig. 2. Our protocol, which takes advantage of our former report [22], was devised as a slight variation of the amidation method of Bulpitt and Aeschlimann [29], who used EDC together with NHS as effective amidation catalyst. As for these authors, we found that the addition of NHS to EDC and an amidation at neutral pH was critical to avoid the formation of the detrimental stable N-acyl urea instead of the desired amide product. Indeed, thanks to NHS the amidation reaction proceeds toward the formation of a stable active ester intermediate that presents as substantial resistance against hydrolysis. In the present case, the coupling reaction was achieved in aqueous media under stirring, with a typical addition of 2.5 mmol amine/1 mmol AGU. The pH of the suspension was adjusted to 7.5–8 with 0.5 M HCl and this pH was maintained throughout the reaction time by adding 0.5 M HCl or 0.5 M NaOH solutions. EDC and NHS with ratios of 1.5 relative to the AGU [22] diluted in 2 mL of water were added. The suspension was stirred during 24 h at 50 °C and finally coagulated by adding an excess of ethanol. After filtration on a 0.5 μm membrane and washing with ethanol (3 times), the precipitate was re-dispersed in water, evaporated again to remove any trace of ethanol, re-suspended in water and finally freeze-dried.

2.2. Characterization

2.2.1. Conductimetric titration

The degree of oxidation or carboxyl groups content of cellulose samples was determined by conductimetric titration [28]. Each dried cellulose sample (50 mg) was dispersed into 15 mL of 0.01 M HCl solution. After 10 min of stirring, a stable suspension was obtained and titrated with 0.01 M NaOH.

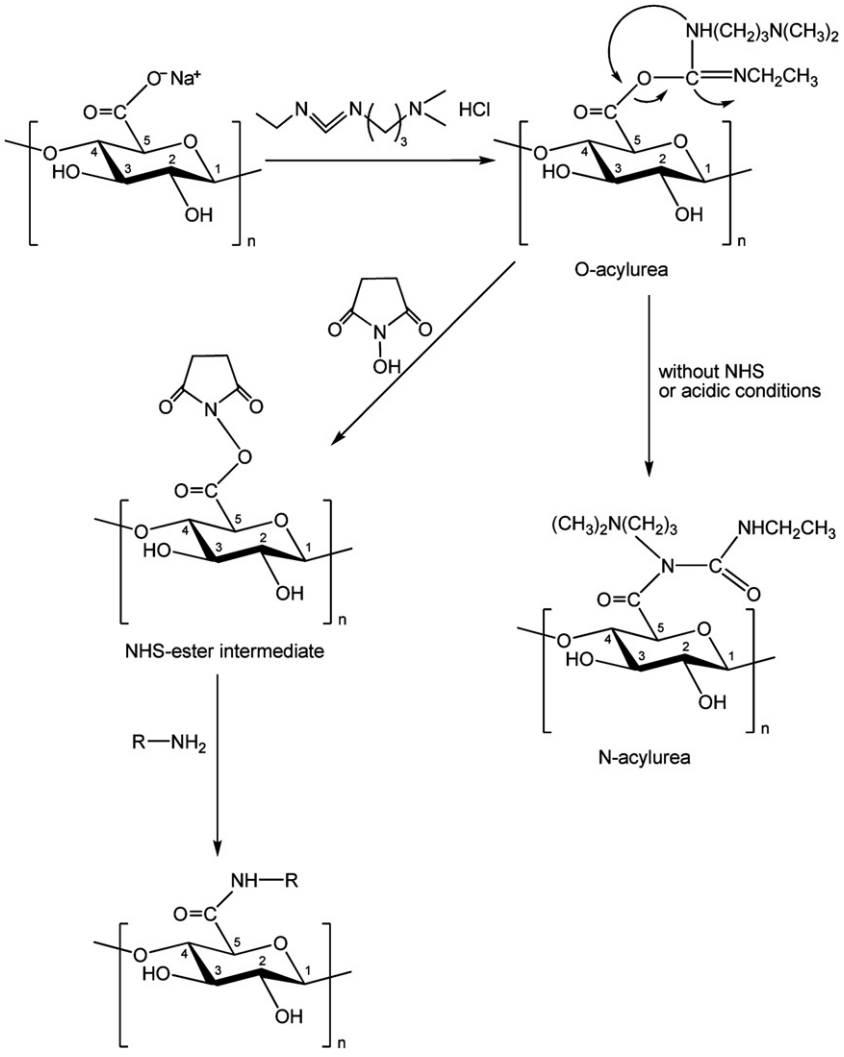

Fig. 2. Coupling reaction by amidation of the surface carboxylated cellulose nanocrystals.

The titration curves, exemplified in Fig. 3, indicate the presence of a strong acid corresponding to the excess of HCl and a weak acid corresponding to the carboxylate content.

The carboxyl groups content *Do* of carboxylated cellulose samples before coupling is given by:

$$Do = \frac{162 \times n_{COONa}}{m - 36 \times n_{COONa}} \quad (1)$$

After the coupling reaction, the residual carboxyl groups content Do_1 is determined by:

$$Do_1 = \frac{[(162 + (Ma - 4) \times Do)] \times n_{COONa}}{[m + (Ma - 40)] \times n_{COONa}} \quad (2)$$

162 (g/mol) corresponds to the molar mass of an uncoupled AGU unit,
M_a the molar mass of 4-amino TEMPO (171.26 mol/L),
m the weight of oven-dried sample (g) and
n_{COONa} (mol) the mole number of carboxyl groups determined by the conductimetry:

$$n_{COONa} = (V_2 - V_1) \times c \quad (3)$$

where V_1 and V_2 are the equivalent volumes of NaOH (in L) and c is the exact concentration of NaOH solution (mol/L).

The degree of conversion (*DC*), which represents the number of coupled AGU, is deduced by the following equation: $DC = Do - Do_1$.

2.2.2. Infrared spectroscopy

Infrared spectra were recorded on an FTIR Perkin–Elmer 1720X spectrometer. Samples were studied as KBr pellets (1% in anhydrous KBr). Spectra were recorded using 3600 cm^{-1} spectral width (between 400 and 4000 cm^{-1}), 2 cm^{-1} resolution, and 32 scans were accumulated. Samples were studied as acidic form to avoid the superposition of sodium carboxylate peak with hydrogen bonds. For this, few milligrams of sample were suspended in 1 mL of water, 1–2 drops of 1 M HCl were added and after stirring during 3–5 min the suspension was centrifuged and the precipitate was washed several times with water until neutrality.

2.2.3. Solid-state ^{13}C NMR spectroscopy

The NMR experiments were performed with a Bruker Avance 400 WB spectrometer operating at a ^{13}C frequency of 100.62 MHz using the combined technique of proton dipolar decoupling (DD), magic angle spinning (MAS) and cross-polarization (CP). ^{13}C and ^{1}H field strengths of 100 kHz were used for the matched spin-lock cross-polarization transfer. The spinning speed was set at 12,000 Hz for all the samples. The contact time was 2 ms, the acquisition time 30 ms and the recycle delay 4 s. The deconvolution of the spectra was achieved following an earlier procedure [24]. The position and width of the lines were maintained constant throughout a series of samples. The area corresponding to the integration of the C1 signal was set to one. The evaluation of the oxidation and degree of crystallinity was made from the integration of the corresponding deconvoluted lines.

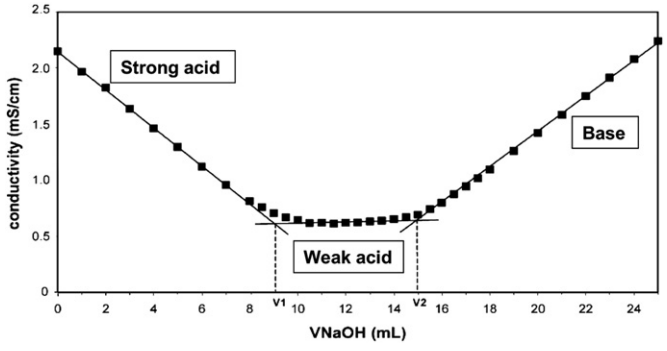

Fig. 3. Typical conductimetric titration curve of oxidized cellulose nanocrystals sample[22].

2.2.4. Electron paramagnetic resonance (EPR) spectroscopy

EPR measurements were made with a Bruker EMX X-band continuous wave spectrometer equipped with a Bruker ER 4116 DM rectangular cavity operating at 9.658 GHz. Experiments were performed at room temperature (300 K) with a hyper frequency power of 1 mW and a modulation amplitude of 0.5 G. The amplitude of the magnetic field modulation and microwave power were adjusted so that no line-shape distortion was observable. The received gain was 63,200 and the sweep time was 42 s. Absolute quantification was obtained by comparison with a TEMPO sample of known concentration after double integration of EPR spectra.

Samples (2 mg), i.e. 4-amino TEMPO and carboxylated cellulose nanocrystals-4-amino TEMPO, were dispersed in H_2O (1 mL) and loaded into a closed capillary tube (o.d. 0.7 mm) which was introduced in a standard EPR tube (o.d. 3 mm).

In order to determine the degree of conversion from EPR data, the average molecular weight M of a glycosyl unit from the cellulose crystal-4-amino TEMPO derivative was calculated as follows:

$$M = 198 \times Do_1 + (162 \times (1 - Do)) + (158 + Ma)(Do - Do_1)$$
$$M = 36 \times Do + 131 \times DC + 162 \quad (4)$$

where

162 (g/mol) corresponds to the molar mass of an unreacted AGU,
198 (g/mol) to the molar mass of oxidized fraction in sodium salt of cellulose (–COONa),
$(158 + Ma)$ to the molar mass of glycosyl unit coupled to 4-amino TEMPO (Ma = 171.26 g/mol),
Do, Do_1 and *DC* represent the degrees of oxidation and the degree of conversion, respectively.

The number of 4-amino TEMPO ($n_{\text{4-amino TEMPO}}$), coupled with cellulose nanocrystals, was issued to:

$$n_{4-\text{amino TEMPO}} = \frac{DC \times m}{M} \quad (5)$$

which gives

$$DC = \frac{(-36 \times Do - 162) \times n_{4-\text{amino TEMPO}}}{131 \times n_{4-\text{amino TEMPO}} - m} \quad (6)$$

where m corresponds to the fraction of the sample in suspension which was introduced into the capillary tube.

2.2.5. X-ray diffraction analysis

X-ray measurements were made on dried pellets of cellulose products. The X-ray diagrams were recorded on a Warhus vacuum flat plate X-ray camera mounted on a Philips PW 1720 X-ray generator operated with Cu Kα radiation at 20 mA and 30 kV. Diffraction images were converted into 2θ-intensity profiles using specific software.

2.2.6. Elemental analysis

The nitrogen content of the coupled samples was deduced from elemental analysis. The analysis of this content was used to verify the degree of conversion (*DC*). The relation between the nitrogen content and *DC* is given in the following equation:

$$DC = \frac{36 \times Do + 162}{\frac{14 \times 100}{\%N} - M_a + 40} \quad (7)$$

where %N corresponds to the nitrogen content of the coupled samples determined by elemental analysis, 162 (g/mol) to the molar mass of an AGU and M_a is the molar mass of 4-amino TEMPO (171.26 mol/L).

3. Results

3.1. Oxidized cellulose nanocrystals

As explained in earlier studies, the TEMPO-mediated oxidation of native cellulose (cellulose I) leads to a biphasic product consisting of a water-soluble and a water-insoluble fraction [27,28]. The former corresponds to a totally oxidized polyglucuronic acid, whereas in the latter only the surface of cellulose nanocrystals is carboxylated. In the present case, the evolution of the *Do* and the yield of the oxidation for the two types of nanocrystals as a function of the amount of the oxidizing NaOCl are presented in Fig. 4. In this figure, one see that the yield of oxidized cellulose samples reaches 92–95% in the case of cotton linters nanocrystals and 88–92% from microfibrillated PCC from SBP.

Remarkably these values were obtained for one equivalent of NaOCl per AGU and there is almost no change in the *Do*, or in the oxidation yield when higher NaOCl contents were used. The fact that the oxidation reaction is stabilized with only one NaOCl equivalent as opposed to the expected two if all the hydroxymethyl groups had been oxidized, is a clear indication of the partial surface carboxylation of the sample. This partial oxidation is corroborated by the measurements resulting from the conductimetric titrations, which give a carboxyl content of 0.15 for the cellulose nanocrystals from cotton linters and 0.21 for those from SBP. The occurrence of surface carboxyl groups is further revealed by the occurrence of an FTIR signal at 1730 cm^{-1} and a ^{13}C NMR resonance at 174.8 ppm.

3.2. Coupling of the oxidized cellulose with 4-amino TEMPO and characterization

In the coupling reaction by amidation process, the reaction yields reached 90–98% for the nanocrystals from cotton linters and 65% for those of microfibrillated PCC from SBP. For the latter, the lower yield can be explained by considering that there is a partial degradation of the coupling product, which is more important when there is a high percentage of a soluble residue. In addition, the small lateral size of the nanocrystals from SBP renders them more difficult to recover quantitatively. The results from the various characterizations, which were used here, are summarized in Table 1.

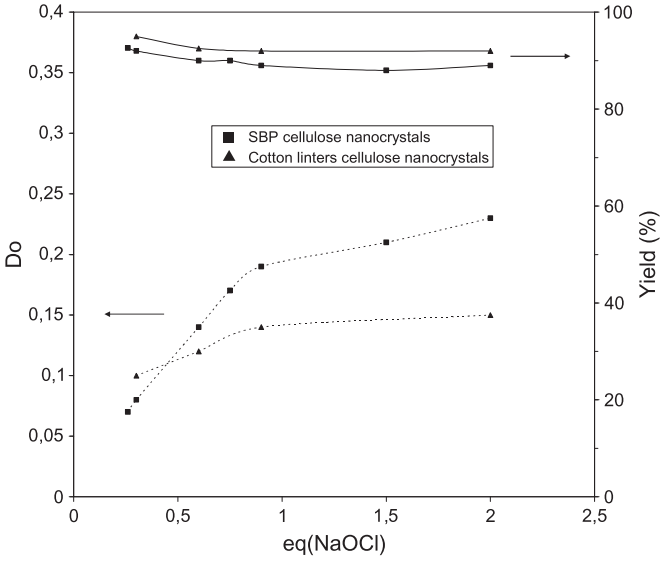

Fig. 4. Evolution of degree *Do* (…) and yield of oxidation (–) versus the amount of added NaOCl.

3.2.1. Conductimetry and elemental analysis

When using these two independent techniques and using the aforementioned equations (3) and (7), there is a remarkable concordance in the values of the *DC* for each of the coupled products. A slight difference is noted between the products, the coupling on the cotton linter nanocrystals being slightly better than that on the SBP nanocrystals: 31% on the former and 26% on the latter. This reduction can be correlated to the decrease in crystal size when going from the cotton linters to the SBP nanocrystals and to the accessibility of the not perfect cellulose crystals. Indeed, with nanocrystals of smaller widths, the possibility to couple molecules at their surface is reduced.

3.2.2. FTIR spectroscopy

Figs. 5 and 6 present the infrared spectra of coupled cellulose nanocrystals. The FTIR spectra of cellulose nanocrystals in acidic form show characteristic strong absorption bands near 3340–3338 cm^{-1} assigned to the (OH) stretching band and near 2900 and 1640 cm^{-1} attributed respectively to (–CH) stretching vibration belonging to the AGU and water molecules adsorbed onto the surface of carboxylated nanocrystals. The strong stretching vibration C=O from free COOH occurs near 1730 cm^{-1} [30–32]. In the spectra of cellulose nanocrystals-4-amino TEMPO conjugates, the carboxyl acid peak occurs near 1726–1728 cm^{-1} and shows a significantly reduced intensity compared with that of the uncoupled products. Two other distinct bands near 1630–1640 and 1550 cm^{-1} are also observed, located in the zone related to the (–CONH–), corresponding to the (C=O) stretching band (amide I) and to the (–NH) bending vibration band (amide II), respectively [33]. These two vibration peaks indicate that an amide bond has been formed between the carboxylic acid in C6 of cellulose and the $-NH_2$ amine end group of 4-amino TEMPO. Indeed, the carboxylic acid peak at 1726–1728 cm^{-1} is well separated from the amide group (–CONH–) bands at 1640 and 1550 cm^{-1}, as already reported by several authors [29,34,35]. In agreement with our present results, Araki et al. [20] have also observed two absorption bands at 1657 and 1544 cm^{-1} corresponding to amide I and amide II absorptions resulting from the effective binding of PEG–NH_2 onto rod like cellulose microcrystals.

A significant reduction in the intensity of the free (COOH) stretching vibration band (1730 cm^{-1}) is also noted in comparison with the spectra of uncoupled oxidized nanocrystals confirming a reduction of the number of (–COOH) functions. This result confirms the chemical modification occurring at the C6 carbon (Figs. 5 and 6).

In examining the spectra, in Figs. 5 and 6, it can be noted that the 3340–3338 cm^{-1} peak are reduced in the spectra of both coupled cellulose samples. This observation is consistent with the occurrence of amide group (–CONH–) bands and supports the formation of the amide link. We can also observe that the intensity of the 800 cm^{-1} peak assigned to (–CH–) bending vibration band (δ_{C-H}) is slightly higher in the spectra of the coupled sample than in the reference one. This difference can be attributed to the presence of (–CH–) groups on the 4-amino TEMPO molecule. Thus our FTIR results confirm the conductimetric and elemental analysis data. The assumption of the presence of uncoupled amine inside the cellulose nanocrystals, increasing artificially the value of *Do*, can be refuted by the presence of characteristic absorption bands of amide groups on cellulose nanocrystals. Similar observations were made

Table 1
Degrees of conversion between surface carboxylated cellulose nanocrystals and 4-amino TEMPO.

Substrates	Degree of conversion (%)*				
	Weight yield (%)	From Conductimetry	From elemental analysis	From EPR analysis	From NMR measurements
Surface carboxylated cotton linter cellulose nanocrystals	98.1	31	32	28	30
Surface carboxylated SBP cellulose nanocrystals	65.2	26	27	24	28

*Accuracy ± 2%.

when polyglucuronic acid in solution was used as starting material for coupling with 4-amino TEMPO [22].

3.2.3. EPR spectroscopy

Electron Paramagnetic Resonance (EPR) spectroscopy has been shown to be a reliable technique to characterize and quantify the microstructural and dynamic properties of various species. Nitroxyl spin labels have been widely used as probes to obtain information about the nature of localized molecular properties such as conformation, flexibility and solute–solvent interactions in diverse systems such as gels, liquid crystals, vesicles, nucleic acids, lipids and proteins [36–39].

The EPR spectra of surface carboxylated cotton linter cellulose nanocrystals-4-amino TEMPO, surface carboxylated SBP cellulose nanocrystals-4-amino TEMPO and an aqueous solution of 4-amino TEMPO as standard reference are presented in Fig. 7. These spectra contained three well-resolved derivatives of Lorentzian lines satisfactorily explained by the Kivelson theory [40]. These three symmetrical lines or triplet are generally characteristic of the presence of free radicals in solution.

For the aqueous solution of 4-amino TEMPO, the general shape of the EPR spectrum is characteristic of the fast motion of a radical, while for conjugate spectra, the lines broadening (particularly the lines at high field) clearly show a decrease in the radical correlation time (Fig. 7). This decrease can be attributed to the restrictive motion of the spin label linked to a polymer-based substrate. It is therefore an indication that the nitroxide moiety has been successfully coupled with the cellulose nanocrystals.

Irwin and collaborators reported that when plant homogalacturonans, either in solution or as solid suspensions were reacted with a carbodiimide reagent in the presence of a paramagnetic nucleophile, the nitroxyamide EPR powder patterns were significantly broadened when as few as 2.5% of the carboxyl functional groups had been labeled [41]. This broadening effect was the same for reactions occurring either in solution or in the solid state. The same behavior can be observed in the cellulose nanocrystals-4-amino TEMPO conjugate spectra for both SBP and cotton linter celluloses. It may be noted that the broadening effect is more pronounced for a product based on cotton linter cellulose than that based on SBP cellulose, confirming that the coupling is more important with cotton linter cellulose than with SBP cellulose.

By double integration (area) of the labeled nanocrystals spectra, we could obtain the absolute number of coupled radicals and thus the fraction of labeling along the cellulosic chain. Thus, the degree of conversion can be calculated. The *DC* values, presented in Table 1, namely 28% for the cotton linters sample and 24% for the SBP counterpart, are very slightly lower than those resulting from conductimetric titrations and elemental analysis.

3.2.4. Solid-state ^{13}C NMR spectroscopy

After HCl hydrolysis, TEMPO-mediated oxidation and coupling reaction, the resulting cellulose nanocrystals samples were characterized by solid-state NMR spectroscopy and the CP-MAS ^{13}C

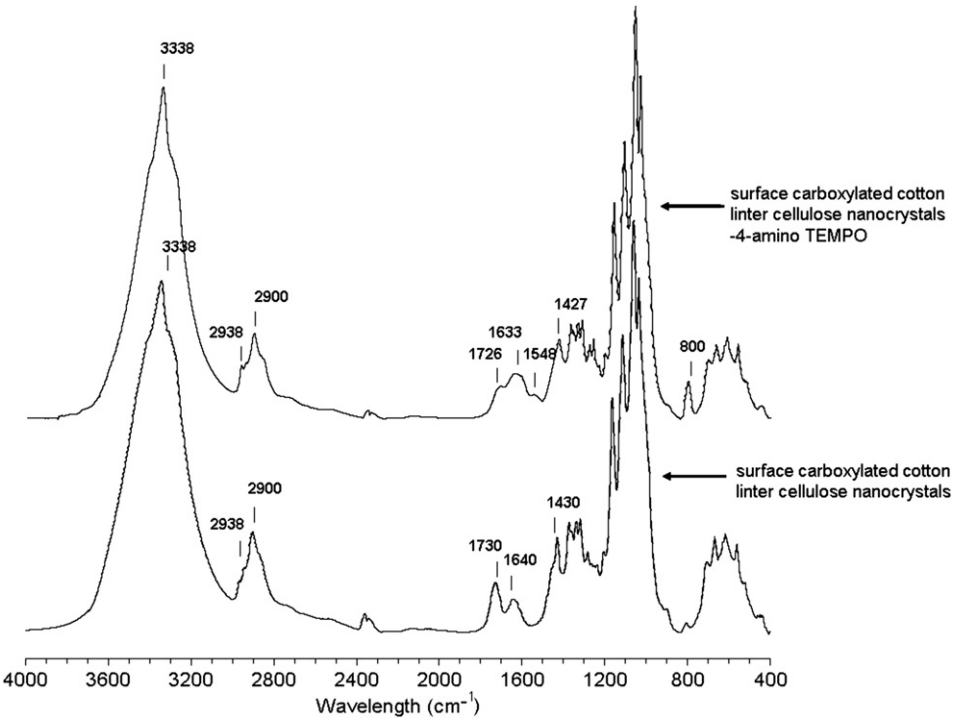

Fig. 5. FTIR spectra of surface carboxylated cotton linter cellulose nanocrystals before (bottom) and after (top) coupling with 4-amino TEMPO.

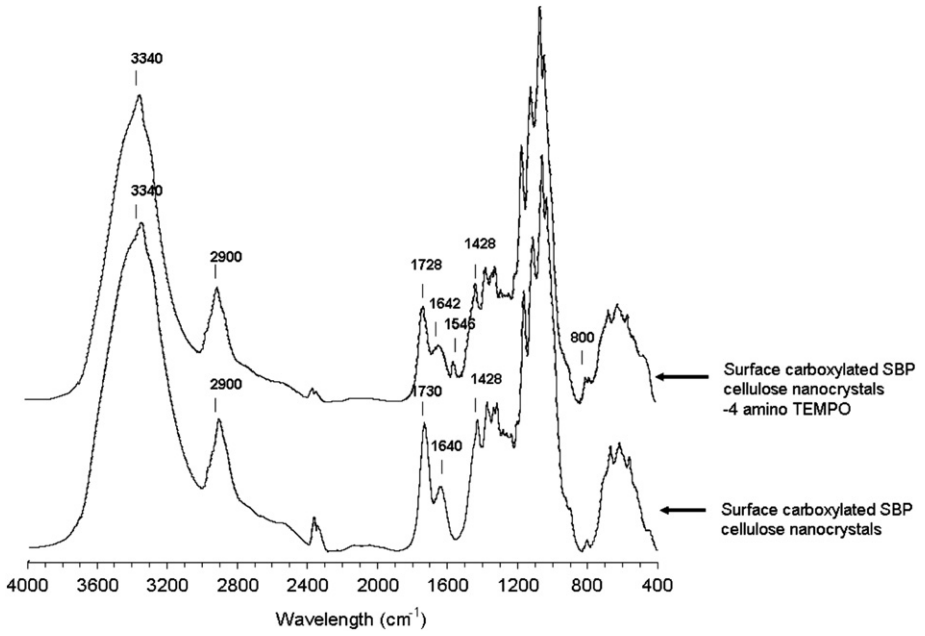

Fig. 6. FTIR spectra of surface carboxylated cellulose nanocrystals from PCC from SBP before (bottom) and after (top) coupling with 4-amino TEMPO.

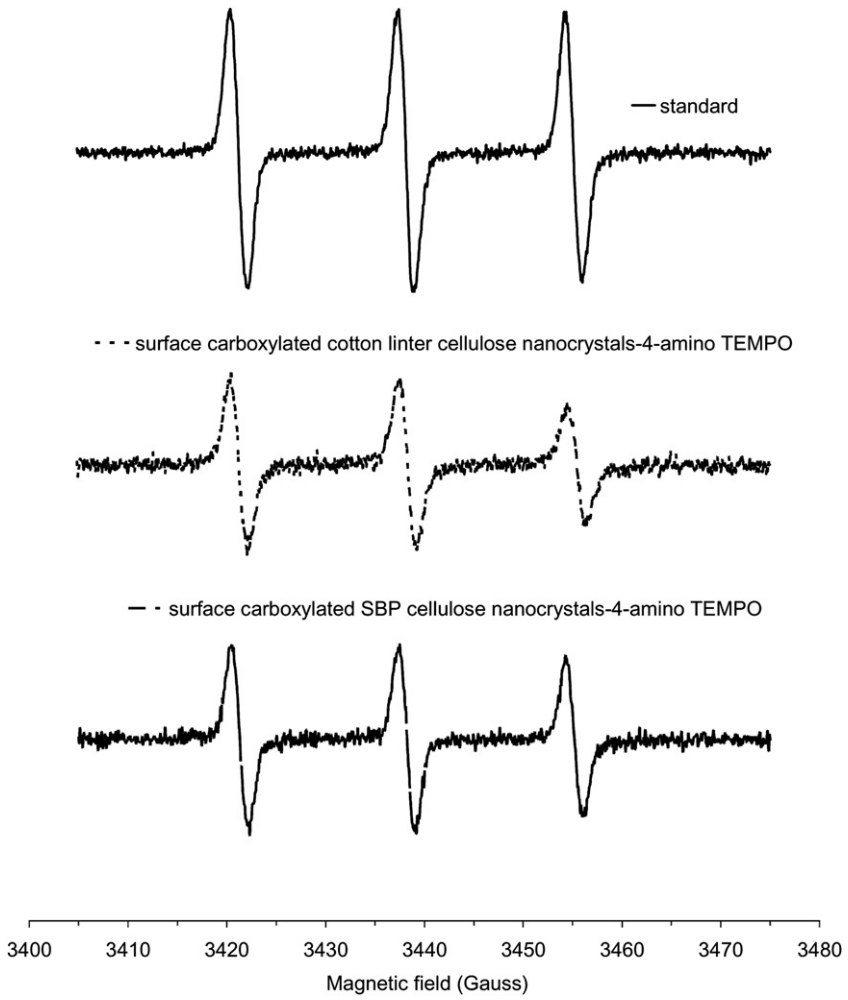

Fig. 7. EPR spectra of 4-amino TEMPO (standard) with surface carboxylated cotton linter cellulose nanocrystals-4-amino TEMPO and surface carboxylated PCC from SBP cellulose nanocrystals-4-amino TEMPO.

NMR spectra are reported in Figs. 8 and 9. The ^{13}C NMR spectra of initial cellulose samples present the characteristic signals of cellulose I [24,26,42–46]. They display two resonances at 62.5 and 65 ppm assigned to disordered and crystalline regions of C6 carbons of cellulose, respectively and between 70 and 77 ppm in the form of two very intense peaks the resonances assigned to C2, C3, and C5 carbons. The signals at 83.5 and 88.7 ppm are attributed to disordered and crystalline regions of C4 carbons, respectively. The last resonance resulting from the C1 carbons of cellulose structure is located at 105 ppm [26,46,47]. When comparing the spectra of the cotton linters and SBP nanocrystals, one notices that the contribution to disordered region at C4 and C6 is higher for the SBP sample. This observation is in agreement with the lower crystallinity and/or crystallite size of the SBP [24].

After oxidation, the major change is the appearance of the carboxyl moiety signal at 174.8 ppm (Figs. 8 and 9), which displays high amplitude. Indeed, as previously observed with the calculation of *Do* by conductimetry, elemental and EPR analysis, the amplitude of the carboxyl resonance signal is higher for SBP sample than for the cotton linter sample, thus revealing a higher *Do* value (Figs. 4, 8 and 9). At the same time, one observes a decrease in the intensity of the signal at 62.5 ppm, corresponding to the carbons of the primary hydroxyl groups (C6) of the disordered regions (Figs. 8 and 9), whereas the crystalline contribution at 65 ppm remains constant. These

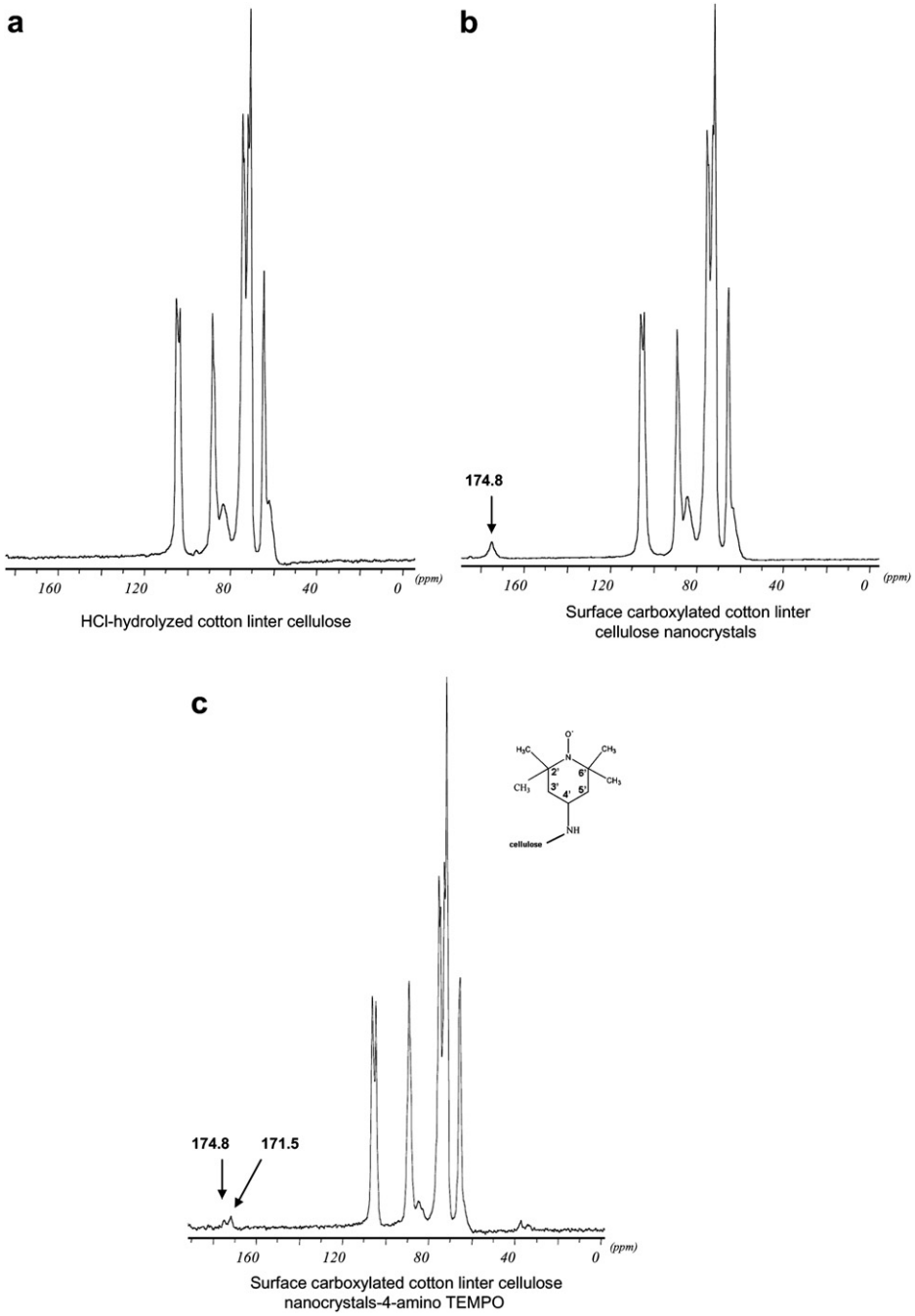

Fig. 8. CP-MAS ^{13}C NMR spectra of (a) hydrolyzed cotton linter samples, (b) surface carboxylated cotton linter cellulose nanocrystals and (c) surface carboxylated cotton linter cellulose nanocrystals-4-amino TEMPO.

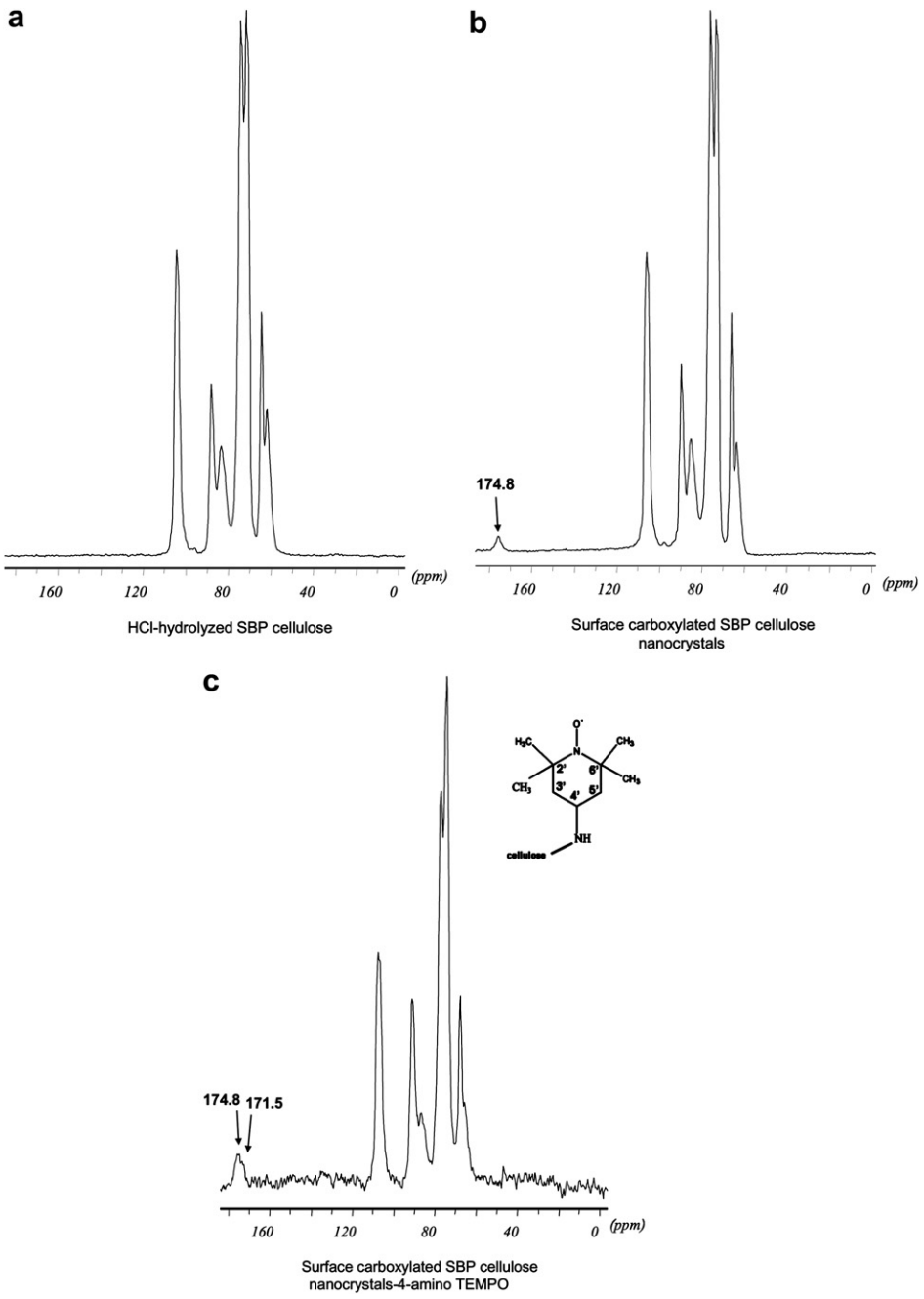

Fig. 9. CP-MAS ^{13}C NMR spectra of (a) hydrolyzed SBP samples, (b) surface carboxylated SBP cellulose nanocrystals and (c) surface carboxylated SBP cellulose nanocrystals-4-amino TEMPO.

indications reveal that only the primary hydroxyl groups located at the surface and in amorphous domains of these samples are being oxidized. In order to obtain more details, the integration of the most relevant signals has been achieved and reported in Table 2 where the *Do* was calculated from the integration of the signal at 174.8 ppm. A crystallinity index [24] was also estimated by comparing the surface area of the C4 signals at 83.5 and 88.7 ppm, corresponding respectively to the carbons in disordered and crystalline regions.

After amidation coupling, significant observations can be considered (Figs. 8 and 9, Table 2): i) the presence of characteristic carbons signals at 40 ppm corresponding to the C3′, C5′ and C4′ of 4-amino TEMPO, ii) the notable reduction of resonance due to the disordered regions of C6 carbons (62.5 ppm), iii) the strong reduction in intensity of the signal at 83.5 ppm attributed to disordered regions of C 4 carbons, and iv) the decrease of the carboxyl moiety signal of carboxylated nanocrystals at 174.8 ppm. The C5 carbons resonance at 77 ppm presents a reduced intensity after coupling, revealing a change in spatial environment due to the coupling at C6 carbons. In addition, a new resonance is detected at 171.5 ppm, well separated from the (−COONa) C6 resonance (174.8 ppm). Based on the aforementioned results [22,32,41], this new resonance corresponds to (−CONH−) acetamide carbon resulting from the coupling of 4-amino TEMPO on carboxylated nanocrystals. For the preparation of the amidated poly(galacturonic acid) with the primary amine group of 4-amino TEMPO, Irwin et al. [41] attributed the signal at 171 ppm to amidated C6 carbons. In addition, resonances located at 40 ppm are equally detected and assigned to C3′, C5′ and C4′of 4-amino TEMPO [22,41].

Table 2
Results of the quantitative analysis of CP-MAS ^{13}C NMR spectra.

Cellulose samples	NaClO (molar ratio)[a]	C=O[b] (174.8 ppm)	C6 *cryst*[c] (68–63 ppm)	C6 *amor*[c] (63–58 ppm)	C6 *total*[d] (68–58 ppm)	C4 *cryst*[c](*CI*[e]) (91–86 ppm)	C4 *amor*[c] (86–81 ppm)
hydrolyzed cotton linter cellulose	0	0	0.68	0.22	0.90	0.75	0.25
surface carboxylated cotton linter cellulose nanocrystals	1	0.10	0.68	0.13	0.81	0.72	0.28
surface carboxylated cotton linter cellulose nanocrystals-4-amino TEMPO	1	0.07	0.68	0.09	0.77	0.72	0.19
hydrolyzed SBP cellulose	0	0	0.54	0.38	0.92	0.52	0.51
surface carboxylated SBP cellulose nanocrystals	1	0.21	0.53	0.27	0.80	0.52	0.48
surface carboxylated SBP cellulose nanocrystals-4-amino TEMPO	1	0.15	0.53	0.22	0.75	0.50	0.48

[a] Mol NaClO/mol AGU.
[b] Carboxyl groups (*DO*) obtained by integration of the signal at 174.8 ppm.
[c] Crystalline and amorphous contents determined by deconvolution.
[d] Obtained by integration of the signal at 62.4 ppm.
[e] Crystallinity index.

Table 2 reveals that the carboxyl group content decreases with the coupling of 4-amino TEMPO. At the same time, a remarkable decrease of the C6 carbons resonance at 62.5 ppm corresponding to the disordered part is observed after coupling, whereas the crystalline contribution at 65 ppm remains constant. This observation, already mentioned in the literature for the TEMPO oxidation process of cellulose [26], is a strong indication of the selectivity of oxidation on primary hydroxyl groups, which occurs only at the surface of nanocrystals and/or in the disordered regions of the cellulose sample. In the amidation reaction, the decrease of the signal at 62.5 ppm, concomitant with a constant contribution at 65 ppm confirms that the coupling of 4-amino TEMPO occurs in the disordered regions of C6 carbons. The decrease of the C4 signal of the disordered regions at 83.5 ppm corroborates this observation.

Indeed, the crystallinity index *CI* has not evolved during the coupling reaction (Table 2): about 0.72 and 0.50 for surface carboxylated cotton linter and SBP cellulose nanocrystals, respectively. This result reflects that the integrity of the crystallites is not altered by the amidation. Furthermore, the solid-state NMR data are a strong indication of the location of amine coupling. The amidation carrying out between the carboxylic acid in C6 of cellulose and the $-NH_2$ end group of amine, the reaction is only realized in oxidized areas. By referring to the cellulose unit cell defined by Sugiyama et al. [50] and according to current models and recent works [26,48,49], it is assumed that the cellulose microfibrils present square section with exposed surfaces opposed to the core of the microfibrils which is considered to be in a crystalline arrangement. This difference between surface and core chains clearly evidenced by solid-state ^{13}C NMR spectroscopy (where different resonances at C4 are attributed either to the core or surface cellulose chains [24,50]) allows to distinguish accessible surfaces located at the exterior of microfibrils aggregates and inaccessible surfaces located inside the microfibrils aggregates. This organization in aggregates is not modifying by HCl hydrolysis that only converts microfibrils into nanocrystals. Regarding the description of the (110) and $(\bar{1}10)$ crystal surfaces [50], the oxidation took place only one-half of the surface hydroxymethyls of cellulose (accessible surface) whereas the other half being toward the core of the crystalline domains. Indeed, Table 2 reveals the presence of carboxylic moiety signal concomitant with a decrease of primary hydroxyl group signal in amorphous domains (at the surface) whereas the crystalline contribution at 65 ppm remains constant. This result indicates that only the primary hydroxyl groups are oxidized and that this oxidation occurs only in the disordered regions of the surface cellulose sample, as previous published [26,50]. The oxidation being carried to the surface of cellulose elements, the amidation coupling therefore occurs at the surface in the disordered regions of the cellulose nanocrystals.

A good agreement with the *Do* values obtained by conductimetry, elemental analysis and EPR spectroscopy is noted. But the coupling occurs with 30% of carboxyl groups suggesting that only one-third of the sites are accessible to the coupling. In addition, one also observes the lower degree of conversion for SBP cellulose than for cotton linter cellulose.

The solid-state NMR data confirm the coupling of cyclic amine 4-amino TEMPO on the surface carboxylated cellulose nanocrystals. In addition, the presence of acetamide carbon on the conjugate induce modifications in environment of C4 and C6 carbons in term of change in disorder, which are observed by a reduction in the intensity of corresponding resonances at 62.5 and 83.5 ppm.

3.2.5. X-ray diffraction analysis

The X-ray diffraction profiles of cellulose nanocrystals-4-amino TEMPO conjugates, together with those of oxidized cellulose references are presented in Figs. 10 and 11. In Fig. 10, the profiles of the oxidized cotton linter cellulose nanocrystals before and after amidation are nearly the same, indicating that the amidation reaction is not affecting the crystalline part of the sample. In fact these patterns are also nearly identical to the pattern of the initial cotton linters or that of their nanocrystals resulting from the hydrolysis. Fig. 11 corresponds to the profiles of the nanocrystals from SPB, before and after amidation. With the exceptions of two strong and narrow peaks that correspond to crystalline impurity – likely calcium oxalate – these patterns are nearly identical to those reported in the literature for SBP cellulose where the calcium oxalate crystals have been removed [23]. As in the case of Fig. 10, there is no visible difference between the sample before and after amidation, but the overall crystallinity of the SPB sample is definitely lower than that of the sample from cotton linters origin: this is revealed by the merging of the (110) and $(\bar{1}10)$ diffraction lines that could be separated in the sample from cotton linters.

The fact that the X-ray diffraction patterns of the amidated and oxidized samples are nearly the same is in full agreement with the results from ^{13}C solid-state NMR results and confirms again that the coupling with 4-amino TEMPO takes place at the disordered regions of the samples that are localized at their surface.

3.2.6. Observation of hydrophobic character

When dispersed in water, the surface carboxylated cellulose nanocrystals led to birefringent suspensions observed between crossed polarizers that did not flocculate or sediment, due to their polyelectrolyte character created by the presence of surface

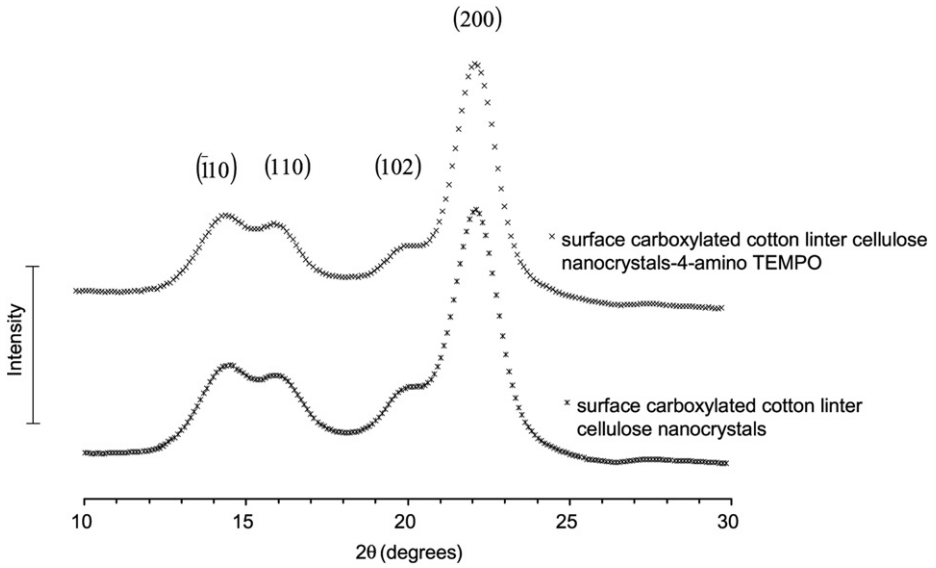

Fig. 10. X-ray diffraction profiles of surface carboxylated cotton linter cellulose nanocrystals and surface carboxylated cotton linter cellulose nanocrystals-4-amino TEMPO conjugate.

negative charges. The effective coupling of 4-amino TEMPO resulted in a drastic change in the stability of suspension, especially against solvents (Table 3).

Due to their surface amidation, the nanocrystals become readily dispersible in organic solvents of low polarity such as THF without aggregation. They form a stable suspension and show flow refringence viewing between crossed polarizers. So these coupled nanocrystals present a lower polarity while maintaining a certain hydrophilic character, certainly due to the small length of amine used. The electron micrographs of the surface carboxylated cellulose nanocrystals (not presented here) reveal well individualized nanocrystals with sharp contours (both at their side and at their tips) and diameters of the order of 4–5 nm for cotton and 3–4 nm for SBP samples, similar to those reported earlier [26]. The surface carboxylated samples show much better dispersion due to the electrostatic repulsion of the negatively charged carboxyl groups located at the surface of the nanocrystals. And, for coupled samples, we can notice that the morphology does not change with nanocrystals presenting the same size and shape with any aggregation.

4. Discussion

The location of amine coupling is clearly evidenced by characterizations by solid-state NMR spectroscopy and X-ray diffraction in this work. Our results indicate that during the amidation reaction, about one-third of the initial carboxyl groups located at the surface of the nanocrystals surface could be amidated. This result is in line with other studies describing the amidation of surface oxidized cellulose nanocrystals with various amines [20,21,30]. In these studies, conversions as low as 4% were found for amidation with hydrophobic amines presenting either a long alkyl chain or an aromatic moiety, whereas a conversion of up to 20% was obtained with low molecular weight PEG–NH_2. At first glance, the reason for this moderate reactivity could originate from the fact that the reaction is achieved on solid substrates, where surface steric hindrance could prevent the correct approach of an amine reagent for successful coupling. However, this may not be the case since the reaction yield between soluble polyglucuronic acid and 4-amino TEMPO was also of the order of nearly one-third [22]. In fact it is

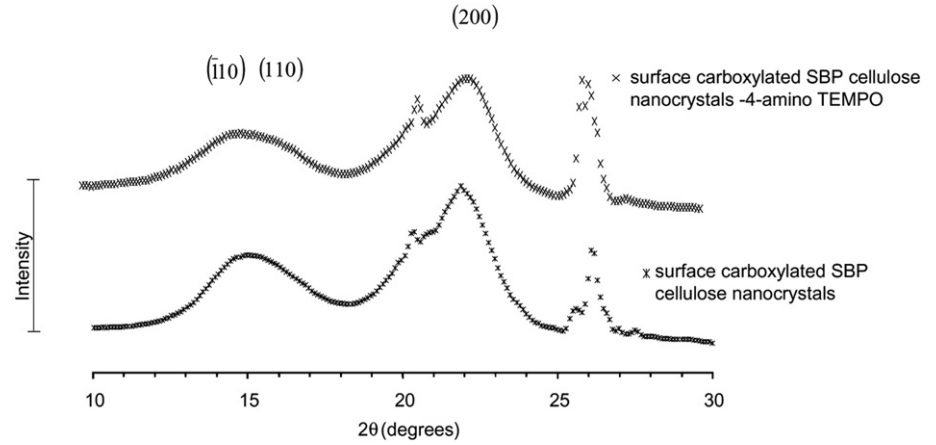

Fig. 11. X-ray profiles of SBP cellulose nanocrystals and SBP cellulose nanocrystals-4-amino TEMPO conjugate. The two sharp peaks at 20.2 and 26° correspond to crystalline impurities, likely calcium oxalate.

Table 3
Results of dispersibility in solvents at ambient temperature.

Samples	Chloroform	Toluene	THF
surface carboxylated cotton linter cellulose nanocrystals	–	–	–
surface carboxylated cotton linter cellulose nanocrystals-4-amino TEMPO	Stable	Stable	Stable
surface carboxylated SBP cellulose nanocrystals-4-amino TEMPO	Stable	Stable	Stable

believed that the intrinsic reactivity of carboxylated polysaccharides toward amidation could be connected with the geometry of the linkage that join the glycosyl units together and not on their solid or liquid state behavior. This phenomenon was already noticed by Danishefsky and Siskovic [47]. In fact, polysaccharides connected by β-D linkages, such as hyaluronic acid or chondroitin sulfates, were far less reactive toward amidation than those connected by α-D linkages such as heparin. Carboxylated cellulose consisting also anhydro sugar units linked in β-D system would fall in the same category as hyaluronic acid, for which amidation yields of about one-third has equally been reported.

The surface amidation of cellulose nanocrystals, which is described here, takes advantage of the initial TEMPO carboxylation of the cellulose samples. This modification, which oxidizes essentially the surface hydroxymethyl groups of cellulose nanocrystals, maintains intact the crystalline perfection of the underlying elements. The method has proven to be the best to individualize and disperse cellulose microfibrils into homogeneous aqueous suspensions [51,52]. It is assumed that this method is also well adapted to disperse the cellulose nanocrystals resulting from acid hydrolysis of cellulose microfibrils. For optimum surface amidation of cellulose, the state of dispersion resulting from the preliminary oxidation step is therefore critical, even if the yield of the reaction is only moderate.

Homogeneous suspensions of cellulose nanocrystals and their unique properties are attracting a great interest in many laboratories. The possibility to obtain such suspensions not only in aqueous environment but also in hydrophobic solvents by modifying the nanocrystals surfaces without affecting their inner core is actively searched. The above protocol confirms that amidation appears to be an easy route to modify the surface of cellulose microfibrils or nanocrystals. In particular, the use of amino groups hooked to either long alkyl chains [21] or polyethylene glycol [20] have shown that after amidation cellulose nanocrystals could be homogeneously dispersed into hydrophobic solvents despite lower yields. In the present case, our surface amidated nanocrystals have kept their hydrophilic character. One of the advantages of our study is that the use of the 4-amino TEMPO reagent has allowed us to use EPR data to confirm the extent of surface amidation of the nanocrystals and its yield.

5. Conclusion

In this study, we have successfully grafted a percentage of 4-amino TEMPO on surface carboxylated cellulose nanocrystals from cotton and sugar beet pulp origin. The coupling, which proceeded from an amidation reaction, occurred essentially at the surface of the cellulose nanocrystals. A coupling of around 30% was achieved for cotton carboxylated nanocrystals and slightly less for those from sugar beet pulp.

Evidence of the amidation reaction was obtained from a serie of analysis, using different techniques, namely elemental analysis, ^{13}C NMR, FTIR and conductimetric titration. In addition, these results were confirmed by EPR measurements, taking advantage of the TEMPO moiety attached to the amide bond resulting from the grafting. This amidation did not modify the morphology and the core of the cellulose nanocrystals that kept their crystalline integrity and therefore their high performance properties. The amine coupling brought a low polarity to the cellulose crystals enabling the modification of cellulose suspensions into hydrophobic materials.

Acknowledgments

The authors acknowledge the help of Dr Serge Gambarelli (CEA-Grenoble, DRFMC/SCIB) for the EPR characterization, Michel Trieweiler for NMR analysis and Dr Henri Chanzy for valuable discussion during this work.

References

[1] Chanzy H. In: Kennedy JF, Phillips GO, Williams PA, editors. Cellulose sources and exploitation. Industrial utilization, biotechnology and physico-chemical properties. Chichester: Ellis Horwood Ltd; 1990. p. 3–12.
[2] Brown MR. J Macromol Sci Pure Appl Chem 1996;133:1345–73.
[3] Bayer EA, Chanzy H, Lamed R, Shoham Y. Curr Opin Struct Biol 1998;8:548–57.
[4] Nishiyama YJ. Wood Sci 2009;55:241–9.
[5] Sugiyama J, Harada H, Fujiyoshi Y, Uyeda N. Mokuzai Gakkaishi 1984;30:98–9.
[6] Revol J-F. J Mater Sci Lett 1985;4:1347–9.
[7] Sakurada I, Ito T, Nakamae K. Makromol Chem 1964;75:1–10.
[8] Sturcova A, Davies JR, Eichhorn S. Biomacromolecules 2005;6:1055–61.
[9] Diddens I, Murphy B, Krisch M, Müller M. Macromolecules 2008;41:9755–9.
[10] Samir ASA, Alloin F, Dufresne A. Biomacromolecules 2005;6:612–26.
[11] Smith B, Goudswaard I, Chanzy H, Cartier N. NL Patent 91 01920, 1991.
[12] Favier V, Chanzy H, Cavaillé J-Y. Macromolecules 1995;28:6365–7.
[13] Marchessault RH, Morehead FF, Walter NM. Nature 1959;184:632–3.
[14] Revol J-F, Bradford H, Giasson J, Marchessault RH, Gray DG. Int J Biol Macromol 1992;14:170–2.
[15] Heux L, Chauve G, Bonini C. Langmuir 2000;16:8210–2.
[16] Goussé C, Chanzy H, Excoffier G, Soubeyrand L, Fleury E. Polymer 2000;43:2645–51.
[17] Berlioz S, Molina-Boisseau S, Nishiyama Y, Heux L. Biomacromolecules 2009;10:2144–51.
[18] Saito T, Shibata I, Isogai A, Suguri N, Sumikawa N. Carbohydr Polym 2005;61:414–9.
[19] Habibi Y, Chanzy H, Vignon MR. Cellulose 2006;13:679–87.
[20] Araki J, Wada M, Kuga S. Langmuir 2001;17:21–7.
[21] Lasseuguette E. Cellulose 2008;15:571–80.
[22] Follain N, Montanari S, Jeacomine I, Gambarelli S, Vignon MR. Carbohydr Polym 2008;74:333–43.
[23] Dinand E, Chanzy H, Vignon MR. Food Hydrocolloids 1999;13:275–83.
[24] Heux L, Dinand E, Vignon MR. Carbohydr Polym 1999;40:115–24.
[25] Dinand E, Vignon MR. Carbohydr Res 2001;330:285–8.
[26] Montanari S, Roumani M, Heux L, Vignon MR. Macromolecules 2005;38:1665–71.
[27] Tahiri C, Vignon MR. Cellulose (Dordrecht, Netherlands) 2000;7(2):177–88.
[28] Da Silva Perez D, Montanari S, Vignon MR. Biomacromolecules 2003;4:1417–25.
[29] Bulpitt P, Aeschlimann DJ. Biomed Mater Res 1999;47:152–69.
[30] Zhu L, Kumar V, Banker GS. Int J Pharm 2001;223:35–47.
[31] Lillo LE, Matsuhiro B. Carbohydr Polym 2003;51:317–25.
[32] Jiang B, Drouet E, Milas M, Rinaudo M. Carbohydr Res 2000;327:455–61.
[33] Williams DH, Fleming I. Spectroscopic methods in organic chemistry. Maindenhead, Berkshire: McGraw-Hill; 1966.
[34] Deng Y, Liu D, Du G, Li X, Chen J. Polym Int 2007;56(6):738–45.
[35] Hu F-Q, Zhao M-D, Yuan H, You J, Du Y-Z, Zeng S. Int J Pharm 2006;315:158–66.
[36] Chamulitrat W, Irwin PL, Sivieri LM, Schwartz RN. Macromolecules 1988;21:141–6.
[37] Gaffney BJ, Marsh D. Proc Natl Acad Sci USA 1998;95:12940–3.
[38] Kurad D, Jeschke G, Marsh D. Biophys J; 2004:264–71.
[39] Mchaourab HS, Lietzow MA, Hideg K, Hubbell WL. Biochemistry 1996;35:7692–704.
[40] Kivelson D. J Chem Phys 1960;33:1094–106.
[41] Irwin PL, Sevilla MD, Osman SF. Macromolecules 1987;20:1222–7.
[42] VanderHart DL, Atalla RH. Macromolecules 1984;17:1465–72.
[43] Horii F, Yamamoto H, Kitamaru R, Tanahashi M, Higuchi T. Macromolecules 1987;20:2946–9.
[44] Ek R, Wormald P, Ostelius J, Iversen T, Nystrom C. Int J Pharm 1995;125:257–64.
[45] Klemm D, Philipp B, Heinze T, Heinze U, Wagenknecht W. Comprehensive cellulose chemistry, vol. 1. Weinheim, New York, Chichester, Brisbane, Singapore, Toronto: Wiley-VCH; 1998. 152 pp.
[46] Isogai A, Kato RH. Cellulose (London) 1998;5(3):153–64.

[47] Danishefsky I, Siskovic E. Carbohydr Res 1971;16:199–205.
[48] Atalla RH, VanderHart DL. Solid State Nucl Magn Reson 1999;15:1–19.
[49] Revol J-F. Carbohydr Polym 1982;2:123–34.
[50] Sugiyama J, Vuong R, Chanzy H. Macromolecules 1991;24(14):4168–75.
[51] Saito T, Nishiyama Y, Putaux J-L, Vignon M, Isogai A. Biomacromolecules 2006;7:1687–91.
[52] Saito T, Kimura S, Nishiyama Y, Isogai A. Biomacromolecules 2007;8:2485–91.